X-ray Absorption Spectroscopic Evidence for the Complexation of Hg(II) by Reduced Sulfur in Soil Humic Substances

K. XIA,*,† U. L. SKYLLBERG,‡
W. F. BLEAM,⊥ P. R. BLOOM,§
E. A. NATER,§ AND P. A. HELMKE⊥

*Department of Agronomy, Kansas State University,
2004 Throckmorton, Plant Sciences Center,
Manhattan, Kansas 66506, Department of Forest Ecology,
Swedish University of Agricultural Sciences,
S-901 83 Umeå, Sweden, Department of Soil, Water, and
Climate, University of Minnesota, 1991 Upper Buford Circle,
St. Paul, Minnesota 55108, and Department of Soil Science,
University of Wisconsin–Madison, 1525 Observatory Drive,
Madison, Wisconsin 53706*

Analysis of Hg(II) complexed by a soil humic acid (HA) using synchrotron-based X-ray absorption spectroscopy (XAS) revealed the importance of reduced sulfur functional groups (thiol (R–SH) and disulfide (R–SS–R)/disulfane (R–SSH)) in humic substances in the complexation of Hg-(II). A two-coordinate binding environment with one oxygen atom and one sulfur atom at distances of 2.02 and 2.38 Å, respectively, was found in the first coordination shell of Hg(II) complexed by humic acid. Model calculations show that a second coordination sphere could contain one carbon atom and a second sulfur atom at 2.78 and 2.93 Å, respectively. This suggests that in addition to thiol S, disulfide/disulfane S may be involved with the complexation of Hg(II) in soil organic matter. The appearance of carbon atom in the second coordination shell suggests that one O-containing ligand such as carboxyl and phenol ligands rather than H_2O molecule is bound to the Hg(II). The involvement of oxygen ligand in addition to the reduced S ligands in the complexation of Hg(II) is due to the low density of reduced S ligands in humic substances. The XAS results from this experiment provided direct molecular level evidence for the preference of reduced S functional groups over oxygen ligands by Hg(II) in the complexation with humic substances.

Introduction

Numerous studies have shown that the biogeochemical cycling of mercury (Hg) is coupled to organic matter in the terrestrial and aquatic ecosystems (*1–3*). The strong interaction between Hg and natural organic matter is believed to be one of the contributing factors for the bioaccumulation of Hg in lakes and rivers remote from local sources of Hg pollution across North America and Europe (*2–5*). Natural organic matter has strong affinity for both Hg(II) and MeHg (methylmercury). The adsorptive affinity of Hg(II) on different soil adsorbents is found to be HA > MnO_2 > clay minerals > Fe_2O_3 > SiO_2 (*6, 7*). Compared to Cu(II), Zn(II), and Cd(II), Hg(II) has several orders of magnitude higher affinity for fulvic acid (*7, 8*). Yin et al. (*9*) found a positive correlation between Hg(II) adsorption rate coefficients and soil organic carbon contents in four soils. A negative correlation was found between the Hg(II) desorption rate coefficients and organic carbon contents in the same soils.

Based on indirect experimental evidence, some speculate that sulfur-containing thiol functional groups on natural organic matter are the principle ligands binding Hg(II) and MeHg (*10–13*). The fact that Hg(II) has high affinity for thiol in biological materials has also been used to support the speculation for the complexation of Hg(II) by thiol functional groups in natural organic matter (*14, 15*). Finally, the Lewis acid–base theory further supports this hypothesis. Mercury-(II) is a "soft" Lewis acid and therefore should bind strongly with thiol which is a "soft" Lewis base.

Recent studies (*16, 17*) show that a significant proportion of humic sulfur is in the reduced S oxidation state (e.g. thio, thiol, or sulfide). The amount of reduced S ranges from 10% of total S in a mineral soil humic substance to more than 50% of total S in an aquatic fulvic acid (*16*). The total S contents range from 0.1 to 3.6% in soil humic substances and from 0.5 to 1.43% in aquatic humic substances (*18*).

The amount of reduced S in humic substances is more abundant than the reported natural levels of Hg in the environment (5–25 pM, *19*). For example, water containing 1 mg L^{-1} humic substances would have a mole ratio between reduced S and Hg(II) ranging from 3000 to 44 000. So far, no direct experimental evidence supports the hypothesis that Hg(II) binds to thiol functional groups in natural organic matter.

Synchrotron-based X-ray Absorption Spectroscopy (XAS) technique, a nondestructive method, has been used in obtaining information on the local chemical environments of elements in a variety of geochemical materials (*20–22*). Only recently, this technique was applied in the characterization of trace metal complexation with natural organic mater (*22*). The detailed theory of XAS has been discussed by Teo (*23*). The structural information provided by the extended X-ray absorption structure (EXAFS) includes average interatomic distances as well as the number and chemical identity of the atoms within a 5 Å radius of the atom absorbing the incident X-ray photon.

In this study the coordination environments of Hg(II) bound to humic acid extracted from a soil and the whole soil were investigated for the first time using XAS.

Experimental Section

Sample Preparation. The humic acid (HA) was extracted from an organic soil horizon developed in a 2–5 m wide zone where the groundwater from the upland soils drain into a lowland fen (i.e. a discharge zone). The soil was collected from the Marcell Experimental Forest, Grand Rapid in northern Minnesota. The pH of the soil in 0.001 M $CaNO_3$ was 5.0, and the loss on ignition was 61% of the dry mass. The humic acid was extracted using 0.5 M NaOH under N_2 and separated from the other components in accordance with the methodology described by Swift (*24*).

A quantity of 100 mg HA which contains about 4.4 μmol reduced S (*16*) was added into 2 mL of 0.02 M $Hg(NO_3)_2$ in dilute HNO_3. Excess amount of Hg(II) was added to the HA in order to saturate all the reduced S sites. The suspension

* Corresponding author phone: (785)532-7213; fax: (785)532-6094; e-mail: kxia@ksu.edu.
† Kansas State University.
‡ Swedish University of Agricultural Sciences.
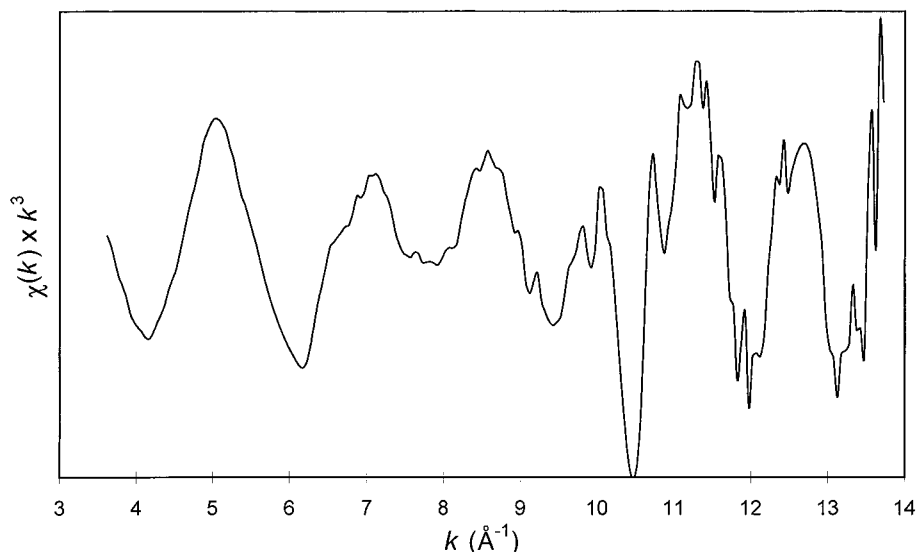§ University of Minnesota.
⊥ University of Wisconsin–Madison.

FIGURE 1. The k^3-weighted EXAFS spectrum for the Hg—humate sample.

was stirred and settled for 2 h and then freeze-dried. The final Hg(II) to reduced S mol ratio in the Hg-humate sample was determined to be 3.1:1.

A soil sample (Hg-soil) adsorbed by Hg(II) was prepared by mixing 0.3 g soil with 100 μmol of Hg(II) in 30.0 mL of a 0.085 M Al(NO$_3$)$_3$ ionic media. The Al^{3+} ionic media was used in order to minimize the release of organic matter from the soil samples during the subsequent Hg(II)-desorption steps. The mixture underwent five desorption experiments (each time resuspended in fresh ionic media) for a total of 1074 h. The sample was then washed five times with 30 mL of distilled water and dried at room temperature. Total digestion of a subsample showed a 92% recovery of added Hg(II). We used the same soil as that for humic acid extraction in this experiment. The Hg(II)/reduced S mole ratio in this sample is about 0.56:1.

Hg L$_{III}$-Edge XAS Spectra Collection and Analysis. Each sample was loaded into a 0.5 mm thick acrylic holder with Mylar film (2.5 μm thick, from Chemplex Industries, New York) windows. All Hg L$_{III}$-edge (12284 eV) X-ray absorption spectra were collected at a bending-magnet beam line (X23A2) at the National Synchrotron Light Source, Brookhaven National Laboratory. Standard operating conditions are 2.58 GeV and 120—200 mA. The monochromator used in these experiments consisted of two parallel Si(111) crystals with an entrance slit of 0.5 mm giving an energy resolution of 2.46 eV at 12 284 eV. Monochromator detuning was unnecessary because high-order harmonics are very weak at the Hg L$_{III}$-edge.

The detector was a Stern-Heald fluorescence ion chamber filled with Kr gas positioned 90 degrees to the incident beam (25). The sample was placed at a 45 degree angle to the incident beam. The L$_{III}$-edge energy was calibrated relative to the energy position of the cleft in the first derivative of pure Hg L$_{III}$ edge. Each XAFS spectrum represents the merged results from four scans. Typical scans ranged from 200 eV below to 600—900 eV above the absorption edge. The preedge background of each merged scan was subtracted, and the absorption coefficient was normalized relative to the absorption threshold.

An EXAFS analysis program, MacXAFS (26) was used in the EXAFS spectra analysis (60—600 eV above the absorption edge). The EXAFS spectra were processed by merging of scans, background removing to isolate the fine-structure scattering curve, and Fourier transformation of the scattering curve to yield a radial structure function (RSF). Background removal involves fitting the pre- and postedge background and

normalization of the edge step. The EXAFS scattering curve was weighted by k^3 (k is the electron wave vector) during background removal and prior to Fourier transformation to enhance damped scattering oscillations. For quantitative analysis, the k^3-weighted EXAFS spectra were Fourier transformed using an unsmoothed window to yield a RSF.

The locations of the peaks in each RSF spectrum represent the distances between the absorber and successive shells of neighboring atoms, uncorrected for phase shift. The amplitudes of the peaks depend on the number and identities of the backscattering atoms. The multiple-scattering X-ray absorption spectroscopy modeling program FEFF-6.0.1 (27, 28) was used in the RSF calculation for the model structure of Hg in humic substances. Each peak in the experimental and FEFF-simulated RSF was then transformed back into k-space (Fourier-filtered) in order to curve fit the experimental results with the predicted results using the fit module in MacXAFS (26).

Results and Discussion

The k^3-weighted EXAFS spectrum for Hg—humate is shown in Figure 1. The irregular peak intensity and frequency of the EXAFS spectrum suggest oscillations from multiple atomic coordination shells surrounding Hg(II).

The Fourier transformed EXAFS spectrum (RSF) shown in Figure 2 provides further evidence of multiple atomic shells surrounding Hg(II). Features in RSF spectrum below 1 Å are due to residual background in the k-space data (29). In the experimental RSF spectrum of Hg—humate, the first and second major peaks appear at 1.6 and 2.1 Å, respectively (Figure 2). Neither peak position was corrected for phase shift. Figure 2 also shows the RSFs of HgO and mercury-thiol compound, Hg(SEt)$_2$. The positions of the phase shift-uncorrected O peak and S peak are at 1.65 and 2.1 Å in the RSF spectra of HgO and Hg(SEu)$_2$, respectively. The matching between the first two peaks of RSF spectrum for Hg—humate with the O peak in HgO spectrum and the S peak in Hg(SEt)$_2$ spectrum provides qualitative evidence that O and S occupy the first coordination shell of Hg in the humate complex.

In addition to the Hg—O and Hg—S peaks, there is a third peak at 2.45 Å in the RSF spectrum of Hg—humate sample. This peak is due to the atoms in the second coordination shell of Hg. The high intensity and broadness of the third peak suggests that an element with an atomic mass (Z) higher than carbon may be present in the second coordination shell. To evaluate this hypothesis, we computed the RSF curves for
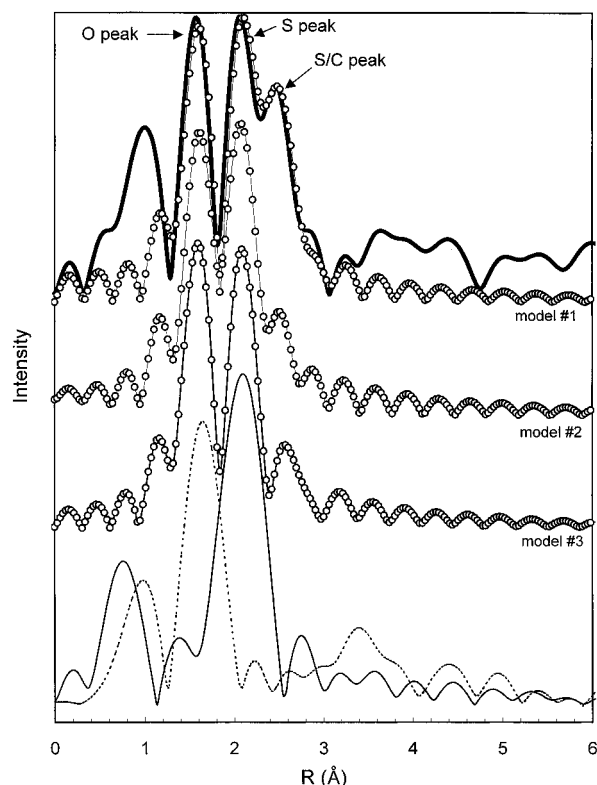
FIGURE 2. Experimental RSFs for Hg(II) complexed with a soil humic acid (heavy solid line) and model compounds, HgO (dotted line), and Hg(SEt)$_2$ (thin solid line). The FEFF-simulated RSFs for the three proposed binding environments of Hg in humic acid (Table 1) are in circled lines. The amplitude reduction factor used in the FEFF calculation is 0.6.

TABLE 1. Three Binding Structure Models for Hg(II)-Humate Used in the FEFF Simulation

models	first coordination shell	second coordination shell
no. 1	1 O at 2.02 Å; 1 S at 2.38 Å	1 C at 2.78 Å; 1 S at 2.93 Å
no. 2	1 O at 2.02 Å; 1 S at 2.38 Å	2 C at 2.78 Å
no. 3	1 O at 2.02 Å; 1 S at 2.38 Å	1 C at 2.78 Å; 1 O at 2.93 Å

three structural models, each with the same first coordination shell (one O at 2.02 Å and one S at 2.38 Å) but with different second shell structures (Table 1) containing various combinations of C, O, and S. The FEFF-computed RSFs for these three models are shown in Figure 2. There is an excellent match in the peak position and peak intensity between the experimental RSF of Hg–humate and model no. 1 containing one S and one C in the second coordination shell of Hg. Notice the low intensity of the third peaks in the other two models. A model (model no. 1) with one O and one S in the first shell and one S and one C in the second shell of Hg most closely matches our experiment results (Figure 2).

Simply matching FEFF-calculated and experimental RSF is not strong validation of the proposed model. A more rigorous test compares the inverse Fourier-filtered scattering curves derived from experimental and simulated RSF curves for each peak. The inverse Fourier-filter of individual RSF peak filters out the interference effects of atoms from other distances. The FEFF-calculated inverse Fourier-filtered scattering curve of a valid model should have the same amplitude, frequency, and phase as experimental filtered scattering curve. A curve-fitting module in MacXAFS (26) was used to fit the inverse-Fourier transformed curve of experimental RSF peak with that of FEFF simulated RSF peak in order to optimize the interatomic distances and the Debye–Waller
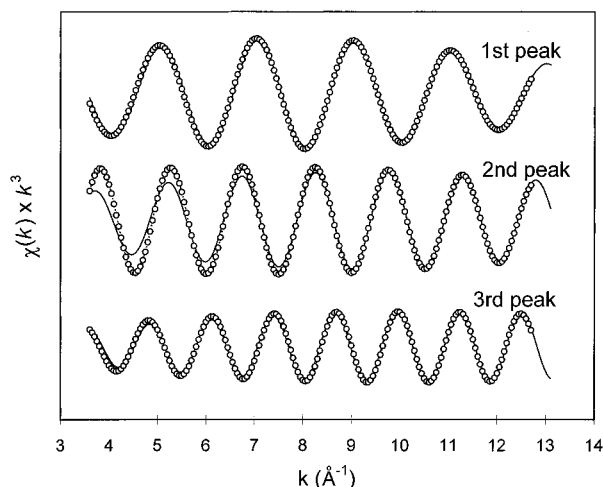

FIGURE 3. Experimental (solid line) and FEFF-fitted (circled line) inverse Fourier transformed scattering curves for the first peak (Hg···O), second peak (Hg···S), and third peak (Hg···S/C) for Hg-humate sample.
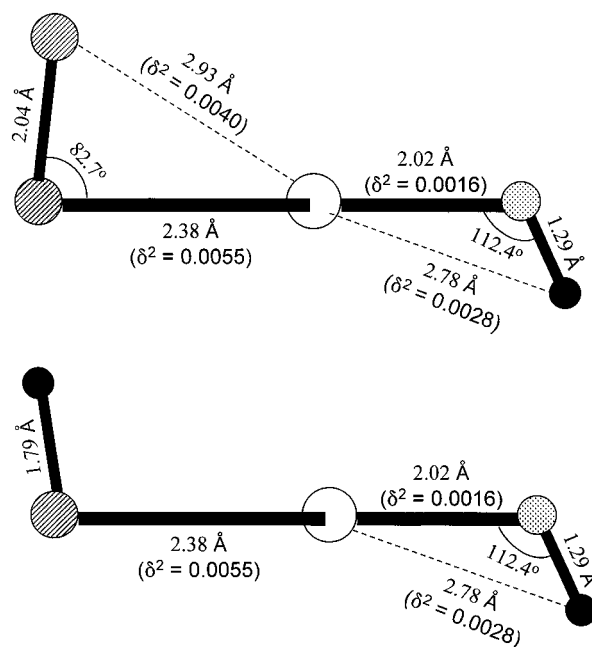

FIGURE 4. Two possible binding structures of Hg complexed with a soil humic acid ((○) Hg, (circle with hatch marks) S, (circle with dots) O, (●) C). Debye–Waller factor (δ) is the root-mean-square distribution (RMSD) of the internuclear distances and represents both dynamic and static disorder. Dynamic disorder arises from vibrations, while static disorder comes from structural and chemical heterogeneity of the substances investigated.

factors for the proposed model. Figure 3 shows the goodness of the fit between FEFF-calculated and experimental inverse Fourier-filtered scattering curves for all three peaks (Hg···O, Hg···S, and Hg···S/C peaks). The proposed binding structures of Hg(II) complexed by humic acid are summarized in Figure 4. The RSF spectrum shown in Figure 2 is a combination of the two possible binding environments. There is one O atom at 2.02 Å (first RSF peak) and one S atom at 2.38 Å (second RSF peak) in the first coordination shell. One C atom at 2.78 Å and one S atom at 2.93 Å appear in the second coordination shell. The broad third peak in the Hg–humate RSF spectrum is a combination of the second shell C atom and the second shell S atom.

The EXAFS results suggest humic acids bind Hg(II) in two-coordinate, having on average a Hg–O bond of 2.02 Å
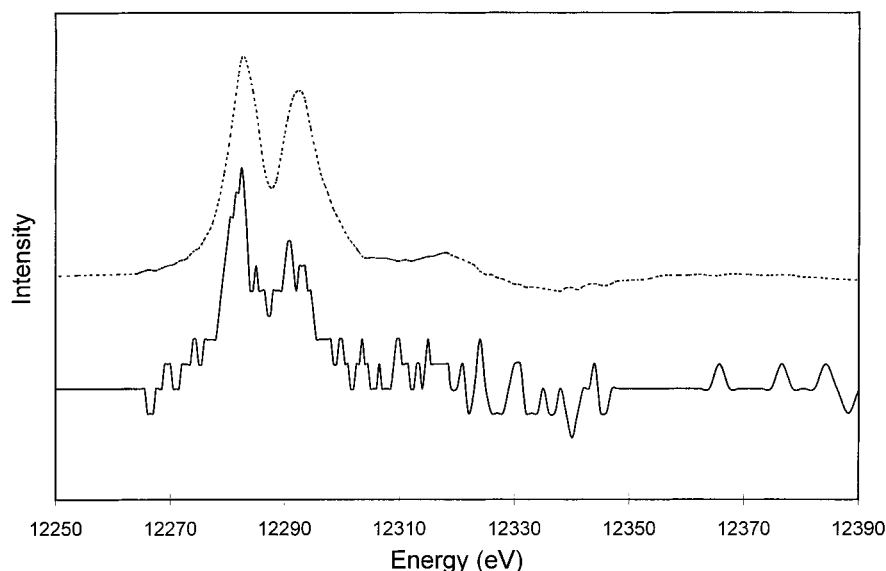
FIGURE 5. First derivative of the X-ray absorption near edge structure (XANES) for Hg—humate (dotted line) and Hg—soil (solid line) samples.

and a longer Hg—S bond of 2.38 Å. A Hg—O bond distance of 2.02 Å is a reasonable value for a two-coordination binding environment of Hg. This value is fairly close to the 2.05 Å distance for Hg—O bond from crystal structure refinement of two-coordinate HgO (orthorhombic) (*30*). The Hg—S distance in humic acid is the same as that found in two-coordinate Hg proteins using EXAFS and in a predicted structure of Hg(SH)$_2$ using a Relativistic Quantum Calculation method (*29, 31, 32*). Furthermore, crystal structure refinement suggests a distance of 2.36 Å for Hg—S bond in two-coordinate HgS (cinnabar) (*30*).

The presence of S atoms at distances of 2.38 and 2.93 Å in the first and second coordination shell of Hg in humic acid is a strong evidence that not only thiol (R—SH) but also disulfide/disulfane (R—SS—R, R—SSH) functional groups in humic acid play an important role in the complexation of Hg(II). Furthermore, because excess of Hg(II) relative to reduced S was added to the humic acid sample, sulfur ligands should not be observed in the immediate binding environment of Hg atom if Hg(II) prefers oxygen ligands over sulfur ligands. The appearance of O together with S in the first coordination shell of Hg is due to two possible reasons. First, because of the large mole ratio between the oxygen ligands and the reduced S ligands (~200:1, using a mean value of 9.7 mmol carboxyl and phenol groups per gram of humic acid (*33*)), once Hg(II) is bond to a reduced S ligand it is more likely for an oxygen ligand rather than a second sulfur ligand to complete the complex at the binding site. Second, since excess amount of Hg(II) was added to the humic acid, it is inevitable that a certain amount of Hg(II) was bonded to oxygen-containing functional function groups such as carboxyl or phenol groups. The EXAFS spectrum of the sample is an average of all the possible binding environments of Hg(II) complexed with the humic acid. Our experimental and theoretical EXAFS results give direct molecular level evidence that Hg(II) prefers reduced S-containing functional groups over other functioning groups in humic acid.

The C atom at a distance of 2.78 Å from Hg atom is more likely from the O-containing functional groups than that from the thiol group, considering the more reasonable bond angle of 112.4° for Hg···O···C than the 80.4° for Hg···S···C in order to satisfy a distance of 2.78 Å for Hg···C (d(C···S) = 1.79 Å, (*34*)). The C atom from the thiol ligand is probably too far out from Hg to be observed in RSF spectrum. The C atom from the disulfide/disulfane ligand (d(S—S) = 2.04 Å and

C···S···S = 104.1°, (*34*)) is at a even longer distance from Hg than that from the thiol group. The appearance of C atom next to O atom in the O ligand rules out the possibility of the binding of Hg by H$_2$O ligand. The small S···S···Hg bond angle (82.7°) is due to the electrostatic attraction of Hg(II) to the S atom in the second shell. A similar bond angle (90.8°) is found for Se···Se···Hg in (PySeSePy)Hg(C$_6$F$_5$)$_2$ (*35*). Two predicted binding structures are shown in Figure 4. One possible structure is the complexation of one disulfide/disulfane ligand and one oxygen ligand with Hg(II). The other possibility is the binding of Hg(II) by one thiol ligand and one oxygen ligand.

The low concentration of Hg in the Hg-soil sample resulted in a high noise level in its XAS spectrum, which made the extraction of the RSF spectrum impossible. However, similarity between the first derivatives of XANES spectra for Hg-soil and Hg-humate samples suggests a similar binding environment of Hg in the whole soil and in its humic acid extract (Figure 5).

The synchrotron-based X-ray absorption spectroscopy reveals the binding structure within the first two coordination shells of Hg in a Hg-humate sample. The presence of S atoms in the first and the second coordination shell of Hg complexed by humic acid is a strong evidence that Hg(II) prefers reduced S functional groups, such as thiol and disulfide/disulfane, in the complexation with humic substances. Because of the large ratio between oxygen ligands and reduced S ligands in humic acids, the density of reduced S ligands is too low for two reduced S ligands to bind Hg(II) simultaneously. Once Hg(II) binds to one reduced S ligand, an oxygen ligand is more likely to bind to the Hg atom in order to complete the complex at the binding site. The low density of reduced S ligands in humic acids explains the appearance of one oxygen atom in the first coordination shell of Hg. Sulfur XANES would not distinguish thiol and disulfide/disulfane ligands in humic substances. The preference of both type of ligands by Hg(II) makes it possible to use Hg(II) as a probe to determine whether thiol and disulfide/disulfane ligands in humic substances react differently with other inorganic or organic ligands.

Literature Cited

(1) Hurley, J. P.; Krabbenhoft, D. P.; Babiarz, C. L.; Andren, A. W. Cycling processes of mercury at the sediment-water interface in seepage lakes. In *Environmental Chemistry of Lakes and Reservoirs*; American Chemical Society: Washington, DC, 1994; pp 425−449.

(2) Mierle, G.; Ingram, R. *Water Air Soil Pollut.* **1991**, *56*, 349−357.

(3) Driscoll, C. T.; Blette, V.; Yan, C.; Schofield, C. L.; Munson, R.; Holsapple, J. *Water Air Soil Pollut.* **1995**, *56*, 499−508.

(4) Meuleman, C.; Leermakers, M.; Baeyens, W. *Water Air Soil Pollut.* **1995**, *80*, 539−551.

(5) McMurtry, M. J.; Wales, D. L.; Scheider, W. A.; Beggs, G. L.; Dimond, P. E. *Can. J. Fish. Aquat. Sci.* **1989**, *46*, 426−434.

(6) Reimers, R. S.; Krenkel, P. A. *Water Pollut. Control Fed.* **1974**, *46*, 352−365.

(7) Xu, H.; Allard, B. *Water Air Soil Pollut.* **1991**, *56*, 709−717.

(8) Lövgren, L.; Sjöberg, S. *Water Res.* **1989**, *23*, 327−332.

(9) Yin, Y.; Allen, H. E.; Huang, C. P.; Sparks, D. L.; Sanders, P. F. *Environ. Sci. Technol.* **1997**, *31*, 496−503.

(10) Benes, P.; Havlik, B. In *The Biogeochemistry of Mercury in the Environment*; Nriagu, J. O., Ed.; Elsevier/North-Holland Biomedical Press: 1979; pp 175−202.

(11) Dyrssen, D.; Wedborg, M. *Anal. Chim. Acta* **1986**, *180*, 473−479.

(12) Dyrssen, D.; Wedborg, M. *Water Air Soil Pollut.* **1991**, *56*, 507−519.

(13) Schuster, E. *Water Air Soil Pollut.* **1991**, *56*, 667−680.

(14) Carty, A. J.; Malone, S. F. In *The Biogeochemistry of Mercury in the Environment*; Nriagu, J. O., Ed.; Elsevier/North-Holland Biomedical Press: 1979; pp 433−479.

(15) Benes, P.; Havlik, B. In *The Biogeochemistry of Mercury in the Environment*; Nriagu, J. O., Ed.; Elsevier/North-Holland Biomedical Press: 1979; pp 175−202.

(16) Xia, K.; Weesner, F.; Bleam, W. F.; Bloom, P. R.; Skyllberg, U. L.; Helmke, P. A. *Soil Sci. Soc. Am. J.* **1998**, in press.

(17) Morra, M. J.; Fendorf, S. E.; Brown, P. D. *Geochim. Cosmochim. Acta* **1997**, *61*, 683−688.

(18) Steelink, C. In *Humic Substances in Soil, Sediments, and Water*; Aiken, G. R., McKnight, D. M., Wershaw, R. L., Eds.; John Wiley & Sons: 1985; pp 457−476.

(19) D'Itri, F. M. In *Biogeodynamics of Pollutants in Soils and Sediments: Risk Assessment of Delayed and Nonlinear Responses*; Salomons, W., Stiglinai, W. M., Eds.; Springer: New York, 1995; pp 391−402.

(20) Brown, G. E.; Calas, G.; Waychunas, G. A.; Petaiu, J. *Rev. Mineral.* **1988**, *18*, 309−363.

(21) Bertsch, P. M.; Hunter, D. B. *Environ. Sci. Technol.* **1994**, *28*, 980−984.

(22) Xia, K.; Bleam, W.; Helmke, P. A. *Geochim. Cosmochim. Acta* **1997**, *61*, 2211−2221.

(23) Teo, B. K. *EXAFS: Basic Principles and Data Analysis*; Springer-Verlag, Berlin, 1986.

(24) Swift, R. S. In *Methods of soil analysis. Part 3. Chemical methods*; Sparks, D. L., et al., Eds.; Soil Science Society of America Book Series: 5. Soil Science Society of America: Madison, WI, 1996; Chapter 35.

(25) Lytle, F. W.; Greegor, R. B.; Sandsrom, D. R.; Marques, E. C.; Wong, J.; Spiro, C. L.; Huffman, G. P.; Huggins, F. E. *Nucl. Instrum. Methods Phys. Res.* **1984**, *226*, 542−548.

(26) Bouldin, C.; Furenlid, L.; Elam, T. *Physica B* **1995**, *208−209*, 190−192.

(27) Rehr, J. J.; Booth, C. H.; Bridges, F.; Zabinsky, S. I. *Phys. Rev. B* **1997**, *49*, 12347−12350.

(28) Zabinsky, S. I.; Rehr, J. J.; Ankudinov, A.; Albers, R. C.; Eller, M. J. *Phys. Rev. B* **1994**, *52*, 2995−3009.

(29) Jiang, D. T.; Heald, S. M.; Sham, T. K.; Stillman, M. J. *J. Am. Chem. Soc.* **1994**, *116*, 11004−11013.

(30) Wells, A. F. In *Structural Inorganic Chemistry*; Claredon Press: Oxford, 1975; p 923.

(31) Raybuck, S. A.; Distefano, M. D.; Teo, B. K.; Orme-Johnson, W.; Walsh, C. T. *J. Am. Chem. Soc.* **1990**, *112*, 1983−1989.

(32) Strömberg, D.; Strömberg, A.; Wahlgren, U. *Water Air Soil Pollut.* **1991**, *56*, 681−695.

(33) Sposito, G. In *The Chemistry of Soils*; Oxford University Press: New York, 1989; p 50.

(34) Garcia, J. G.; Haydar, S. N.; Krapcho, A. P. *Acta Crystallogr.* **1995**, *C51*, 2333−2335.

(35) Kienitz, C. O.; Thone, C.; Jones, P. G. *Inorg. Chem.* **1996**, *35*, 3990−3997.